Adaptive Wireless Power Transfer

Michael Loh
Eng. Phys
Final Project Report, 2024-2025
michaelloh@cmail.carleton.ca

Project Supervisor
Dr. Rony Amaya
ronyamaya@cunet.carleton.ca

This project explores an adaptive wireless power transfer system designed to focus energy using phase-controlled antenna arrays. By dynamically adjusting the relative phases of 2.4 GHz patch antennas, the system creates zones of constructive interference to maximize power delivery at specific locations. A receiver equipped with an RF power detector communicates measurements back to a control unit, which uses a particle swarm optimization (PSO) algorithm to tune the phase transmission in real time.

Carleton University

CONTENTS

1 Introduction **5**
1.1 Project Introduction . . . 5
1.2 Literature Review . . . 5
1.3 Problem Statement . . . 6
1.4 Technical Contribution Statement . . . 6

2 Adaptive Wireless Power Transfer System **7**
2.1 Project Objective . . . 7
2.2 Overall Technical and Engineering Challenges . . . 7
2.3 Proposed Approach & Solution . . . 7
2.4 Design Stages . . . 8

3 Phase and Power Simulation **9**
3.1 Principle . . . 9
3.2 Technical Challenges . . . 10
3.3 Important Design Aspects: Features & Limitations . . . 10
3.4 Comparison with State-of-the-art techniques . . . 10
3.5 Alternative Techniques . . . 11

4 Numerical Demonstration **13**
4.1 Design Considerations . . . 13
4.2 Design Implementation . . . 13
4.3 Hardware Setup . . . 16
4.4 Measurement Results . . . 16
4.4.1 Hardware Test 1 . . . 16
4.4.2 Hardware Test 2 . . . 17
4.4.3 Numerical Test 1 . . . 18
4.4.4 Numerical Test 2 . . . 18
4.5 Discussions . . . 19

5 Conclusions **21**
5.1 Summary . . . 21
5.2 Overall Project Contributions and Achievements . . . 21
5.3 Future Work . . . 21

6 Appendix **23**
6.1 Extension from Fall Work Term . . . 23
6.2 Project Resources . . . 23

CHAPTER 1

INTRODUCTION

1.1 Project Introduction

Low-power wireless devices such as passive RFID tags, environmental sensors, or small wearables could make use of ambient energy harvesting, especially in environments where battery replacement is impractical such as nuclear reactors, or medical environments. Use of inductive based energy harvesting has been explored however typical ranges for usable levels of power transfer are very near field with wireless charging of devices occurring within contact ranges. DARPA has invested in the development of Radio Frequency (RF) long range power transfer in order to power devices at long ranges, including powering drones and potential space based power generation systems. The RF regime theoretically allows for power harvesting at much greater distances than inductive based systems and advantages over optical wavelength range systems in environments without clear lines of sight such as through walls or clouds. The motivation of this project was to design and simulate a proof-of-concept for further future development of RF based power transmission technology.

Furthermore within the scope of this project is investigating the implementation of a network of antennas to power devices within a room. These antennas would be able to turn on or off depending on the proximity of the receiver device as well as modify their phase angle to generate a region of local constructive interference to maximize power received.

1.2 Literature Review

In terms of general references that were useful 'Analysis and Design of MHz-range Wireless Power Transfer Systems for Implantable Devices' [1], 'A Critical Review of Wireless Power Transfer via Strongly Coupled Magnetic Resonances' [2], and 'Powering IoT Devices: Technologies and Opportunities' [3] were very useful in exploring the area of wireless power transfer technologies. 'Powering Iot devices' was a useful for guiding potential use cases for the project and for wpt tech in general. The 'Implantable Devices' paper was also very useful for comparing and contrasting various energy harvesting and WPT methodologies such as magnetic inductance and RF transmission. Lastly, the SCMR paper, though targeted at magnetic inductance technology, was useful in beginning the investigation of RF transmission architectures, and relevant components for the design of an RF system, save for an antenna.

In terms of specific articles that have helped with my specific sub component. Circuit Design's 'RF Design Guide' [4], 'Design of a wireless power transfer system using electrically coupled loop antennas' [5], and 'Software-based wireless power transfer platform for various power control experiments' [6] were also very useful. The RF design guide has been quite useful for understanding RF far field propagation as well as relevant performance metrics. The 'Design of wireless power transfer system' was also quite useful for understanding the hardware architecture of RF power systems, and the software based wireless power transfer platform was useful for understanding the MATLAB capabilities for modeling the system.

1.3 Problem Statement

For a transmitter network delivering power, the radiation from all the antennas will interfere to produce power dead zones and peaks. The goal of this project was to adapt the phase angles on the transmitters using phase shifters, to create a region of constructive interference at the receiver. This would be realized through the use of an algorithm that could search for regions of peak power from the measured power data. To implement this algorithm a simulation of the interference generated by the transmitters was setup in order to model the parameter that the algorithm would need to adjust. Furthermore communication between receiver and transmitter would need to be implemented, in this case Bluetooth was chosen as it is readily implementable with micro controllers. To achieve the project goals four teams were setup. Transmitter architecture was handled by Justin Bouwmeister. Receiver architecture was handled by Prabjhot Shaglania. Interference simulation was modeled by Michael Loh (Author). Lastly, algorithm design, and hardware integration was handled by Nathan Gomes.

1.4 Technical Contribution Statement

The overall novel aspects of this project were: the adaptive phase modification to generate peak power, the development of an algorithm for optimizing interference between RF transmitters, and the simulation of a multi-transmitter interference pattern.

First the adaptive phase modification is novel in that many wireless power transfer systems rely on having only one transmitter to couple to. This forces the transmitter and receiver to specific geometries facing each other, often times leading to coupling geometries and proximity that leads to minor improvements over wired connections. Having multiple transmitters in the RF regime allows for a larger range of system geometries as well as longer ranges for measurable power to be transmitted. With multiple transmitters the receiver can be located within a much larger area and still serviced by 1 2 or more transmitters. The main drawback being multiple transmitters operating at the same frequency leads to destructive interference. In our case this is being mitigated by our phase shifting optimization algorithm.

The second novel aspect is the development of a Particle Swarm Optimization algorithm for the shifting of phases on patch antennas. This is a novel implementation of the particle swarm optimization methodology. Other algorithms could have been used however the draw of PSO was the scalability in being able to handle many more than 3 transmitters. Brute force was initially tested and found to have similar convergence times to PSO however as the number of transmitters increased in the simulated system it became too slow.

The authors component (the interference simulation of the transmitter network) served as the training space for the optimization algorithm. This served to test out several algorithms prior to implementation in order to verify that the algorithm would be capable of handling the requirements such as convergence times, repeatability, and capability of handling 3 or more transmitters. Additionally, it also served to train the selected Particle Swarm Optimization (PSO) algorithm prior to hardware implementation.

CHAPTER 2

ADAPTIVE WIRELESS POWER TRANSFER SYSTEM

2.1 Project Objective

The objectives of the project were to design, fabricate and integrate three transmitting patch antennas with phase shifting capability, a receiver patch antenna with rectification and power metering, a receiver to transmitter Bluetooth communication system using micro controllers, the simulation of the phase interference between multiple antennas, and the training and implementation of the phase optimization algorithm on the micro controllers. The critical parameters for the transmitter were a 2.4GHz (2.375GHz) center frequency and below -10db reflection (-25db) at the center frequency. For the rectifier an 80% conversion efficiency was targeted, and for the algorithm and phase simulation the goals were to have phase optimization converge for multiple transmitters.

2.2 Overall Technical and Engineering Challenges

The main engineering challenges were the modeling of the physics involved with EM interference, optimization and design of the patch antennas, and lastly the design and fabrication of the phase shifters.

With the simulation challenges the difficult came from integrating the phase interference of the waves, with the power transmission characteristics of the antennas. With the patch antennas the main challenges arose from the fabrication of the antennas as the listed FR4 dialectric constant on the manufacturer and the simulated FR4 differed leading to changes to the center frequency. With the phase shifters the main challenge was the design and fabrication of the evaluation boards for the desired phase shifting chip. Due to funding problems the prefabricated boards could not be purchased and the phase shifters had to be assembled in house. However due to time constraints they could not be designed and assembled in time.

2.3 Proposed Approach & Solution

Transmitter system uses an RF generator that gets split into 3 signals. The baseline signal goes through the RF amplifier to the transmitter, while the other two lines go first through phase shifters then RF amplifiers before passing into the antenna. The antennas have been matched to 50 Ohms, as well as the other components. On the reciever side the power is read off using the RF power meter, which then communicates with the micro controllers which implement the optimization algorithm and adjusts the relative phases on the transmitters. The cables carrying RF signals are all standard SMA cables capable of carrying a 2.4GHz frequency signal in the power range we were using 0dbm - 20 dbm.

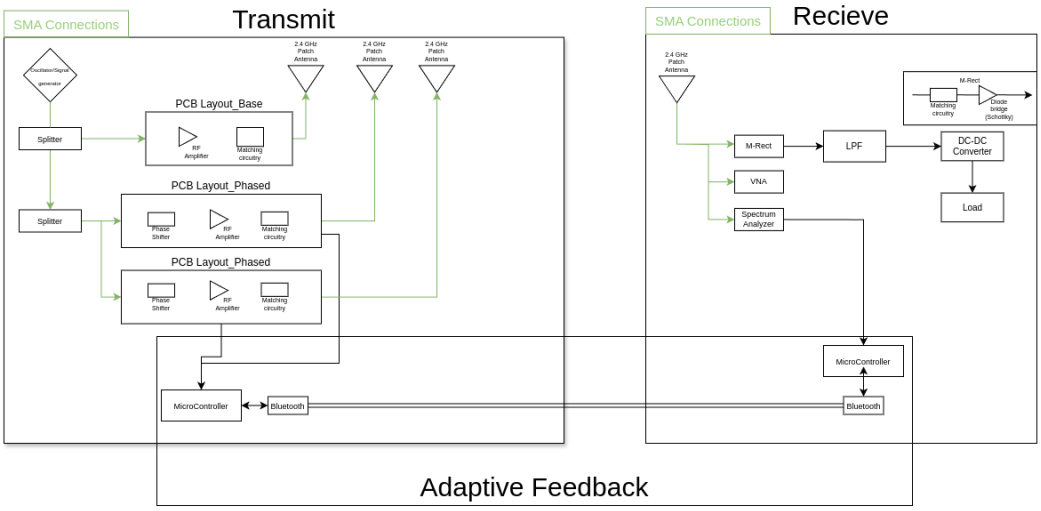

Figure 2.1: System Block Diagram

2.4 Design Stages

Justin Bouwmeister was responsible for the transmitter architecture and patch antenna design. This involved laying out the patch antennas in ADS and getting them fabricated by JLCPCB. As well as designing the overall transmitter architecture with the generator, RF amplifier, phase shifter system connected via SMA cables. Prabhjot Shaglania was responsible for the receiver architecture and rectifier design. Which involved the design of a bridge rectifier for the receiver. Nathan Gomes was responsible for the algorithm development and hardware testing. Which involved the testing and comparison of multiple algorithm methodologies including brute force, gradient, and PSO, as well as training the selected algorithm on the simulated data for implementation on the micro controllers. Furthermore Nathan was responsible for the Bluetooth communication between micro controllers and their integration with the phase shifters. Michael Loh (Author) was responsible for the simulation development. Which included the research and development of the phase and power simulation of the transmitters using the collected data of the fabricated patch antennas.

CHAPTER 3

PHASE AND POWER SIMULATION

3.1 Principle

In order to simulate the optimal power transfer system an understanding of power transfer systems and the physics behind the system are essential. For this project we will be using radio frequency electromagnetic waves as the energy propagating system. These waves will travel in space with changing phase corresponding to a change in time and position. These waves can be modelled in a variety of ways. One common approach is the Yee Cell which separates the magnetic and electric component of the travelling wave vectors, another is the Laplace equation which connects the voltage change at the source to an electrical potential that can change in time. For our purposes we will consider a geometric approach to the problem. For this system we will be observing the interference of three waves. To simplify the system we will assume that each wave will come from a point source, which in the far field regime appears to be acceptable. The phase of each individual point source can be modelled by a spherical plane wave as a solution to the 3D wave equation[7].

$$u(r) = \frac{A}{r} * e^{i(\omega * t \pm k * r)} \tag{3.1}$$

Here u(r) is the wave function, A is the amplitude, ω is the angular frequency = $\frac{f}{2\pi}$, t is time, k is the wave number =$\frac{2\pi}{\lambda}$, and r is the radial direction in spherical coordinates. To note, this hold for monochromatic free space spherical waves, it is also an isotropic representation that models a point source. For non isotropic solutions such as for a dipole antenna higher order effects with angular dependence are required and the spherical harmonics are used. This models a function oscillating in time with frequency and wavelength governed by ω and k. For our setting the EM radiation will interfere in space but not oscillate in time as the frequencies are the same. As can be shown by a linear combination of solutions with same k and omega their time dependence oscillates in time at the same rate thus only the linear combination of both waves at any time t will oscillate in time. ie for constructive interference the amplitude at that point will oscillate with amplitude 2A for all time t. This simplifies the problem as now we can set t to an arbitrary time t = 0, and solve for the phase dependence which only depends on r. Secondly the wave function is of the form of a complex exponential, which from Euler's formula:

$$e^{i\theta} = cos(\theta) + isin(\theta) \tag{3.2}$$

Allows us to use the complex sinusoidal representation.

$$u(r) = \frac{A}{r}(cos(\frac{2\pi r}{\lambda}) + isin(\frac{2\pi r}{\lambda})) \tag{3.3}$$

Next from the intensity equation[8] we can derive a function for A.

$$I = \frac{P}{area} = |u(r,t)|^2 = \frac{A^2}{r^2} \tag{3.4}$$

Thus $\frac{A}{r} = \sqrt{\frac{P}{area}}$ We can then use the Friis equation to get P, and the area will be the smallest simulation length scale as the area 'a'.

$$P_r = P_t * G_t * G_r * (\frac{\lambda}{4\pi r})^2 \tag{3.5}$$

Where Pr is the received power, Pt is the transmitted power, G is the gain of the antenna, λ is the wavelength, and r is the distance between transmitter and receiver.[9] Since we also have the directive gain of the transmitters from the patch antenna team lead, we can also make G a function of theta. The transmitter and receiver are the same antenna and so share the value of G and we will make the assumption Gt=Gr however with the angle dependence this may not be true in practice as the antennas may not be facing each other at the same angle. Inserting A back into the wave equation we get:

$$u(r) = \frac{\sqrt{(P_t * G(\theta)^2 * (\frac{\lambda}{4\pi r})^2)}}{\sqrt{a}}(cos(\frac{2\pi r}{\lambda}) + isin(\frac{2\pi r}{\lambda})) \tag{3.6}$$

Since the 3D free space wave equation is a linear differential equation any linear combination of solutions is also a solution. Which means our full wave equation for the system becomes.

$$U(r) = \Sigma_{i=1}^{3} u_i(r) \tag{3.7}$$

Subsequently the full intensity of the system becomes:

$$I = |\Sigma_{i=1}^{3} u_i(r)|^2 \tag{3.8}$$

and the power can be recovered as well:

$$P = I * a = |\Sigma_{i=1}^{3} u_i(r)|^2 * a \tag{3.9}$$

Where a will be the area scale for the simulation and P is is the power seen at that point in space.

3.2 Technical Challenges

In terms of technical challenges the main limiting factor was granularity of the simulation as well as simulation accuracy when incorporating physics contributions. As you increase the precision of the arrays, they get larger proportional to a quadratic, ie increasing the array by 100x100 yields 100000 more data points, which Matlab online only supports array sizes up to 5GB so it led to making the grain size of the 1m by 1m simulation space 0.000004^2m. Which is much smaller than the wavelength of 0.1250m. Furthermore implementing the 2D and 3D models involved the integration of multiple physical models, each with their own set of approximations. As a result the overall model only reflects a portion of the overall physics. As adding more layers to the model would have become unwieldy for training the algorithm and also too delayed in the project timeline to give the algorithm team sufficient time to train and test their algorithm.

3.3 Important Design Aspects: Features & Limitations

The main features are the modeling of the phase space of the 3 transmitter system, as well as providing rough estimates for power received. The main limitations derives from the assumptions made. The main assumptions being that the transmitters behave as point sources in the far field, the Friis equation is accurate at 2.4GHz, there are no reflections, and that the receiver can receive isotropically. Overall these limitations make for a rather limited scope of the simulator, however the main goal, which was simulating the phase component was acheived, which allowed for the algorithm to be trained. The phase of the simulation only relies on the assumption that the antennas behave as point sources which appears to be typical for RF applications in the far field regime.

3.4 Comparison with State-of-the-art techniques

Existing techniques such as ANSYS HFSS use FTDT simulations of the EM space which provides a much more accurate power simulation and should give a more accurate phase simulation as well. The goal of the simulation was to build a model that could capture the interference component and though Yee Cells are quite useful they are more complex than this system requires. Using the free space wave equation allows for a quicker overall development time which allowed for the algorithm team to begin testing much earlier.

3.5 Alternative Techniques

Alternative techniques could have involved creating a full system simulation in ANSYS, however this would have taken significantly more time as this would have relied on the antenna team to finish designing and modeling the patch antennas early enough to begin setting up the antenna models in ANSYS in the fall. Which was not the case. Using a mathematical model allowed for much earlier completion of the sub team goals and allowed for the team lead (author) to assist with the other sub teams throughout the winter term. Additional mathematical modelling could have also included higher order spherical harmonics if dipole antennas or other antenna architectures were used. Furthermore, instead of using the Friis approximation other power equations could have been used. Using the Friis appoximation allowed for concurrent testing with the antenna team, which did use the Friis equation.

CHAPTER 4

NUMERICAL DEMONSTRATION

4.1 Design Considerations

The solution to the wave equation was implemented in MATLAB to create a 2D simulation space for the power and interference map. This code was then passed to the algorithm team which then used the simulator to test and train multiple different algorithms (PSO, Gradient Descent, and Brute Force). The choice of Matlab allowed for easy cross-team integration as the algorithm was also being implemented in Matlab.

4.2 Design Implementation

In this section the code for the simulator is broken down into the various simulation steps.

In the first part the necessary sim space variables are setup, including all physical constants, the room bounds, transmitter parameters, and simulation granularity. To add more transmitters, more variables need to be initialized, which could be solved using functions and structs, however for the simple 3 transmitter setup this was sufficient.

```
%constants
f = 2.4*10^9; %frequency
c = 3*10^8; %speed of light in m/s
lda = c/f; %wavelength
N = 500; %granularity
grain = 1/N; %length scale m

%room bounds in m
yM = 1;
ym = 0;
xM = 1;
xm = 0;

%x position offsets of transmitters in m
x1off = 0;
x2off = 0.5;
x3off = 0;

y1off = 0;
y2off = 0;
y3off = 0.5;

%phase offsets in degrees of transmitters
%variable degree of freedom to be controlled by algorithm
poff2 = 0;
poff3 = 0;

%angles the transmitters are facing at
theta1 = pi/4;
theta2 = pi/2;
theta3 = 0;
```

Figure 4.1: Initialization section

In this section the radial distance to each of the transmitters is calculated. This will be used to calculate the wave function from each point source. Here the wave function is listed as 'phasex' and includes the phase offsets to modify the relative phase angles between the wave functions. Additionally, t is set to 0 as we don't need to oscillate in time when we solve for intensity and power.

```
%calculate distance and phase

%x and y vectors
xRx = linspace(xm,xM,N);
yRx = linspace(ym,yM,N);

%calculates radial distance to transmitters at all points in simulated
%space with distance offsets of the transmitter placements
for k = 1:500
    for j = 1:500
        diff1(k,j) = sqrt((xRx(k)-x1off)^2+(yRx(j)-y1off)^2);
        diff2(k,j) = sqrt((xRx(k)-x2off)^2+(yRx(j)-y2off)^2);
        diff3(k,j) = sqrt((xRx(k)-x3off)^2+(yRx(j)-y3off)^2);
    end
end

%calculates phase using the free space wave equation solutions
phase1 = cos(pi/lda*diff1)+1i*sin(pi/lda*diff1);
phase2 = cos(pi/lda*diff2+pi/180*poff2)+1i*sin(pi/lda*diff2+pi/180*poff2);
phase3 = cos(pi/lda*diff3+pi/180*poff3)+1i*sin(pi/lda*diff3+pi/180*poff3);
```

Figure 4.2: Phase and radial distance calculation

In this section the angles projecting from the transmitter are calculated. These angles will later be used to

calculate the directive gain received along each ray.

```
%solving for directive gain

G = table2array(GainVAngle); %imports gain directivity from ANSYS simulation

%calculates transmitter angle projections
for k = 1:500
    for j = 1:500
        angle1(k,j) = atan((xRx(k)-x1off)/(yRx(j)-y1off))-theta1;
        angle2(k,j) = atan((xRx(k)-x2off)/(yRx(j)-y2off));
        angle3(k,j) = atan((xRx(k)-x3off)/(yRx(j)-y3off))-pi/2;

    end
end

angle1(1,1) = 0; %removes atan(0) = nan

% accounts for atan flipping sign past pi/2 for vertically facing
% transmitter
for k = 1:500
    for j = 1:250
        angle3(k,j) = angle3(k,j)+pi;
    end
end
```

Figure 4.3: Transmitter projection angles calculation

This part of the code is used to calculate the 'A' coefficients for each point source wave function as derived in the 'Principle' Section. The coefficient is roughly equal to the square root of the Friis equation. Also notable are the case statements that prevent the transmitter origins from being included as they will be divided by zero cases. Furthermore, the function Gt that outputs the directional gain measured in Ansys is also included in the Appendix.

```
%Calculation of the A coefficients of the wave equations with directive
%gain Gt

pt = 10; %Transmitter power in mW ie 10dbm
for k = 1:500
    for j = 1:500
       if diff1(k,j) ~=0
            A1(k,j) = (pt*Gt(angle1(k,j),G)^2*(lda/(diff1(k,j)*4*pi))^2)^0.5;
       end

       if diff2(k,j) ~=0
            A2(k,j) = (pt*Gt(angle2(k,j),G)^2*(lda/(diff2(k,j)*4*pi))^2)^0.5;
       end

       if diff3 ~= 0
            A3(k,j) = (pt*Gt(angle3(k,j),G)^2*(lda/(diff3(k,j)*4*pi))^2)^0.5;
       end
   end
end
```

Figure 4.4: Calculation of the wave function coefficients 'A' with respect to directive gain

Finally all the parameters are summed to give the intensity function. The equation is of form:

$$I = |A_1(cos(\frac{2\pi r_1}{\lambda}) + isin(\frac{2\pi r_1}{\lambda})) + A_2(cos(\frac{2\pi r_2}{\lambda}) + isin(\frac{2\pi r_2}{\lambda}))A_3(cos(\frac{2\pi r_3}{\lambda}) + isin(\frac{2\pi r_3}{\lambda}))|^2 \quad (4.1)$$

```
% Full wave
I = zeros(500); %Initializing Intensity
P = zeros(500); %Initializing Power

for k = 1:500
    for j = 1:500
       if diff1(k,j) ~= 0 && diff2(k,j) ~= 0 && diff3(k,j) ~= 0
            I(k,j) = (abs( (A1(k,j)/grain)*phase1(k,j) + (A2(k,j)/grain)*phase2(k,j) + (A3(k,j)/grain)*phase3(k,j) ))^2;
       end
       P(k,j) = 10*log10(I(k,j)*grain^2);
    end
end
```

Figure 4.5: Calculation of the total wave function, Intensity, and Power

With additionally, the 'grain' term refers to the area of the unit being calculated which for this simulation is a 0.002m by 0.002m area. Overall the 'grain' term will cancel out and can be neglected in the power output, but was included during testing to ensure that the intensity was accurate in dimension. Additional, code was written to output the plots seen in the later sections, and is included in the appendix.

4.3 Hardware Setup

In terms of test setup the hardware section was only partially completed with the phase shifters unfortunately taking too long to produce. As such the main hardware testing was in the form of patch antenna characterization. The first test measured the power received as a function of distance between the two antennas. This served as a validation of the Friis equation, and also the simulation. The second experiment was that of the directivity of the antennas, measuring the received power as a function of antenna angle, and determining the directive gain.

In terms of numerical tests. The first test involved the simulation of a single antenna, which could be validated against the lab measured results and the Friis equation. The second numerical test was the simulation of the three antennas and verifying that there was regions of constructive and destructive interference.

4.4 Measurement Results

4.4.1 Hardware Test 1

The theoretical power received was calculated using the Friis equation, while the measured power was taken in lab using two patch antennas.

Distance (cm)	Theoretical Power Received [dBm]	Measured Power Received [dBm]
30	-18.85	-21.4
40	-21.35	-23.9
50	-23.289	-26.7
60	-24.87	-27.4
70	-26.21	-28.2
80	-27.37	-28.6
90	-28.39	-29.1
100	-29.309	-31.5
110	-30.137	-31.6
120	-30.89	-31.6
130	-31.588	-32.5
140	-32.23	-33.4
150	-32.83	-33
160	-33.39	-32.9
170	-33.91	-34
180	-34.415	-34
190	-34.88	-34.5
200	-35.33	-34

Figure 4.6: Table of measured power vs distance between antennas at 0dbm

4.4.2 Hardware Test 2

Below summarizes the results of the patch directivity test. The measured column is the data taken in lab. Whereas the simulated gain was done in ANSYS HFSS by the Antenna team. For the simulation, the ANSYS data was used as the lab data was subject to experimental issues with the SMA cables causing unpredictable losses that varied between experimental days.

Angle	Measured Gain (dB)	Simulated Gain (dB)
0	-2.986381521	-0.3339731872
15	-3.486381521	-0.5523857697
30	-4.236381521	-1.462656451
45	-5.486381521	-2.468291371
60	-6.986381521	-4.44268771
75	-7.486381521	-6.280064601
90	-7.986381521	-8.646779285
115	-8.986381521	-12.79427472
130	-9.486381521	-15.90072635
145	-9.986381521	-18.15372046
160	-10.48638152	-18.97936356
175	-10.68638152	-18.77828864
180	-10.98638152	-18.72565504

Figure 4.7: Table of measured power vs angle between antennas at 0dbm

4.4.3 Numerical Test 1

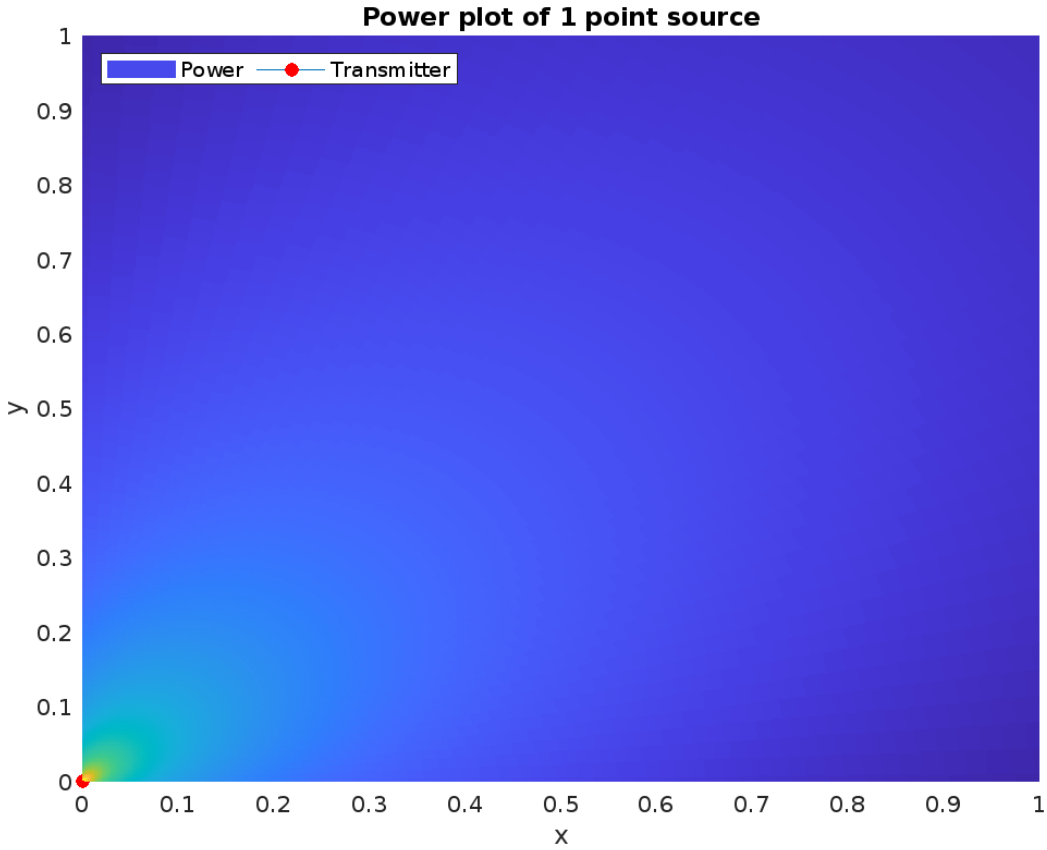

Figure 4.8: Plot of single transmitter simulation

Distance (cm)	Theoretical Power Received [dBm]	Measured Power Received [dBm]	Simulated Power Received (dBm)
30	-18.85	-21.4	-20.1897
40	-21.35	-23.9	-22.6885
50	-23.289	-26.7	-24.6762
60	-24.87	-27.4	-26.2516
70	-26.21	-28.2	-27.6199
80	-27.37	-28.6	-28.7709
90	-28.39	-29.1	-29.7871
100	-29.309	-31.5	-30.7214
110	-30.137	-31.6	-31.5426
120	-30.89	-31.6	-32.2927
130	-31.588	-32.5	-33.0022
140	-32.23	-33.4	-33.6405

Figure 4.9: Table comparing simulation results to measured power and theoretical power vs distance

4.4.4 Numerical Test 2

Below is the plot of 3 point sources interfering in space.

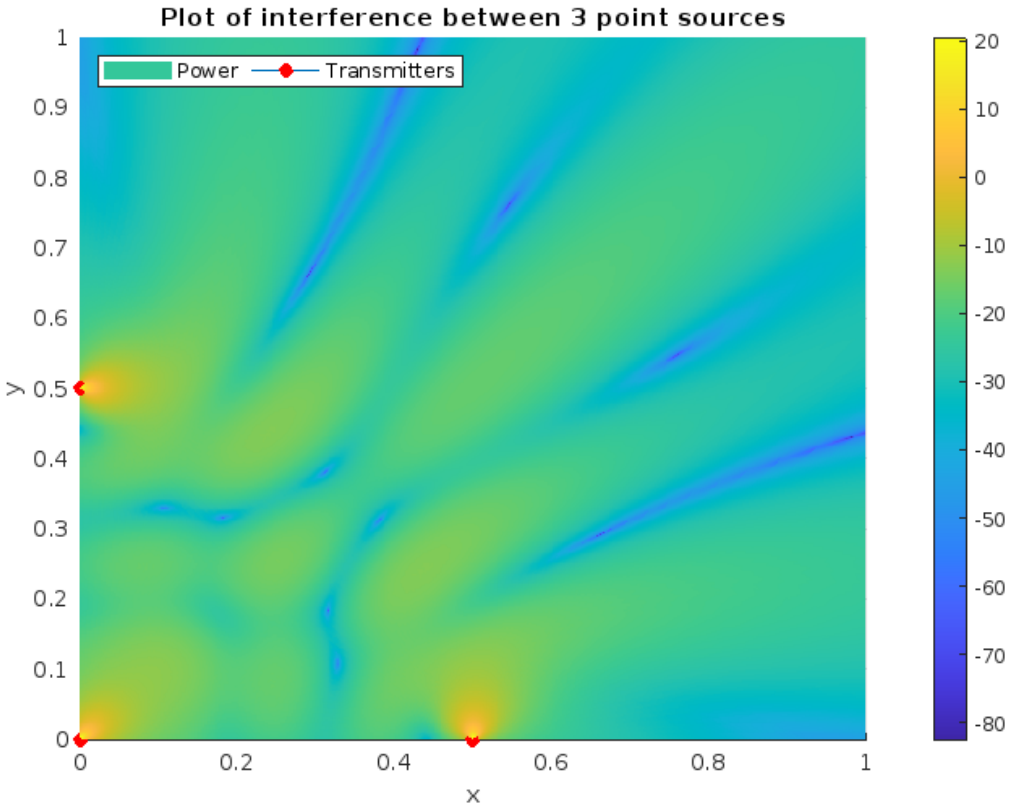

Figure 4.10: Plot of 3 point sources interfering in space

4.5 Discussions

From Hardware Test 1 it demonstrates that the received power appears to follow the Friis equation within the scope of the system. This supports the use of the Friis equation in the simulation as well as validates the antenna gain parameters. In Hardware Test 2 we see the measured and simulated gain with respect to angle. The simulated gain comes from ANSYS HFSS in which the patch team modeled the gain directivity. The measured gain appears to be significantly lower than the simulated gain. This may be due to losses caused by the SMA connectors which appeared to change loss values depending on the angle and geometry of their positioning. This is atypical for SMA wires which, unlike fiber optic cables, should not change their matching or increase in losses due to their orientation. As such in the MATLAB simulation the ANSYS HFSS simulated directivity was used. In Numerical Test 1 a single point source was simulated. The results were then compared to the lab measurements and friis equation results from Hardware Test 1 which appeared to validate the simulation model. Secondly in Numerical Test 2 the full simulation was performed. This demonstrated the constructive, and destructive interference of the system. This would have been compared with the lab measurements however hardware testing was not fully completed, and as such the full simulation could not be verified. Subsequent testing would have been done to verify the locations of the destructive and constructive zones. As well as modeling and testing of the full system with the phase shifters to verify the algorithm in both simulation and hardware

CHAPTER 5

CONCLUSIONS

5.1 Summary

The project began in the fall term with literature review and design of the phase space simulation. In the winter term the power components were introduced to create the full power and phase simulation of the system. The simulation was initially integrated with the algorithm team in the fall as the algorithm testing was able to be performed on the phase components of the point sources alone, whereas in the winter the full integration of the wave equation was integrated with the algorithm team for testing and validation of the algorithm.

5.2 Overall Project Contributions and Achievements

In terms of individual contributions the simulation team successfully developed and integrated a first order wave equation simulation that integrates power directivity, phase, and scalability to various transmitter network setups. The benefit of the simulation to the project was to be able to simulate the power coupling of various setups for the algorithm team to compare, test, and train various algorithm regimes. The main challenges to the simulation were to determine the various physical effects that would have the largest impact on the lab test setup, as well as integrating said physical models into MATLAB.

5.3 Future Work

In terms of future work the most important next step would be to complete the full hardware implementation with the phase shifters, as well as new SMA cables that have predictable losses. Further, testing would be able to be done including further validation of the simulation regime, as well as investigation of additional physics phenomena, such as changes of medium, and reflections. These investigations could guide additional modifications to the simulator that could better capture the possible physical phenomena that could arise in the system. Additional, work could also be done on the antennas. With phase shifters, a phased array antenna with beamforming could be developed instead of the patch antennas. This would provide additional parameters for the algorithm to control as well as additional physical parameters to add to the simulator.

CHAPTER 6

APPENDIX

6.1 Extension from Fall Work Term

In the winter term the main objective was to integrate the power directivity into the simulator. This was achieved using the Friis equation integrating into the wave equation, as well as the directivity measurements made by the antenna team. The initial designs for the code looked much different as the power was initially being integrated separately after the phase components were calculated. However after further investigation and testing it was found that the directive gain could be integrated straight into the wave equation. The main technical differences revolve around the physics simulation methods. Initially only the sin solutions to the wave equation were considered and the full sin cos model was ignored as MATLAB can run into difficulties plotting imaginary numbers. However in the winter plotting the wave equation was set aside for plotting the intensity. This allowed for the full sin cos wave equation to be modeled, and the intensity allowed for the integration and plotting of the power, much more easily.

6.2 Project Resources

	Source	Item Name	Description
1	KEFC	Signal splitter - ADP-SMAM-2SMAF	RF Signal Splitter
2	KEFC	MAPS-010164-TR0500	6 bit phase shifter
3	KEFC	MAX2016EV Kit	RF signal monitoring unit
4	KEFC	Capacitor (Multilayer Ceramic Capacitors MLCC - SMD/SMT)	100pF AC grounding capacitor
5	KEFC	Capacitor (Multilayer Ceramic Capacitors MLCC - SMD/SMT)	10nF (0.01uF) AC grounding capacitor
6	KEFC	Control pin array	2 row - 20 pin header
7	KEFC	SMA jack	0.8mm gap SMA jack
8	KEFC	SeeSii Upgraded TinySA Ultra Spectrum Analyzer	Spectrum Analyzer
9	KEFC	Patch Antenna Fabrication	Fabrication & Delivery of Patch Antenna PCBs
10	KEFC	Phase Shifter PCB Fabrication	Fabrication & Delivery of Phase Shifter PCBs
11	KEFC	Poster	Poster printing for Poster Fair
12	DoE Borrowed	RF Amplifier - ZX60-272LN-S+	RF amplifier
13	DoE Borrowed	Male to Male SMA Adapter	SMA connector
14	DoE Borrowed	Female to Female SMA adapter	SMA connector
15	DoE Borrowed	3 inch male to male SMA cables	SMA cable
16	DoE Borrowed	3ft male to male SMA cabled (one side 90°)	SMA cable
17	DoE Borrowed	2ft male to male SMA cable purple	SMA cable
18	DoE Borrowed	3fr male to male SMA cable blue	SMA cable

Figure 6.1: List of hardware components used

```
function [Gt] = Gt(angle,Gain)


x = int16(abs(angle*180/pi));
if mod(x,2) == 1
    x = x+1;
elseif x == 0
    x = 2;
end

index = find(Gain(:,1)==x);
Gt = Gain(index,2);

end
```

Figure 6.2: Function to find directive gain

```
figure
surf(xRx,yRx,P,LineStyle='none',EdgeColor='none')
hold on

p = plot3(0,0,1,"-o");
p.MarkerFaceColor = [1 0 0];
p.MarkerEdgeColor = [1 0 0];
q = plot3(0,0.5,1,"-o");
q.MarkerFaceColor = [1 0 0];
q.MarkerEdgeColor = [1 0 0];
a = plot3(0.5,0,1,"-o");
a.MarkerFaceColor = [1 0 0];
a.MarkerEdgeColor = [1 0 0];
colorbar

xlim([0 1])
ylim([0 1])
%zlim([0 1])
xlabel('x')
ylabel('y')
title('Plot of interference between 3 point sources')
legend({'Power','Transmitters'},'Location','northwest','Orientation','horizontal')

hold off
```

Figure 6.3: Plotting code for simulator

Angle	Gain (ratio)	Angle	Gain (ratio)	Angle	Gain (ratio)
0	0.9259822914	64	0.3375796912	128	0.0312413759
2	0.9255875411	66	0.3186836495	130	0.02860100312
4	0.9230964146	68	0.3005169274	132	0.02622111039
6	0.9185315841	70	0.283084597	134	0.02409023926
8	0.9119326344	72	0.2663865364	136	0.02219662695
10	0.9033554023	74	0.2504180318	138	0.02052814342
12	0.8928710658	76	0.2351703729	140	0.0190722472
14	0.8805650072	78	0.220631434	142	0.01781596167
16	0.8665354778	80	0.2067862326	144	0.01674587295
18	0.8508920976	82	0.1936174616	146	0.01584815014
20	0.8337542242	84	0.1811059879	148	0.01510858812
22	0.8152492297	86	0.1692313147	150	0.01451267261
24	0.7955107228	88	0.157972005	152	0.01404566665
26	0.7746767542	90	0.1473060619	154	0.01369271708
28	0.7528880406	92	0.137211267	156	0.01343897907
30	0.730286242	94	0.1276654743	158	0.01326975616
32	0.7070123202	96	0.1186468601	160	0.01317065293
34	0.683205007	98	0.1101341303	162	0.01312773668
36	0.658999402	100	0.1021066846	164	0.01312770456
38	0.6345257173	102	0.09454474186	166	0.01315805197
40	0.6099081817	104	0.08742942549	168	0.01320723803
42	0.5852641112	106	0.08074281454	170	0.01326484388
44	0.5607031497	108	0.07446796099	172	0.01332171976
46	0.536326678	110	0.06858887765	174	0.01337011676
48	0.5122273882	112	0.06309049937	176	0.01340379988
50	0.4884890137	114	0.05795862131	178	0.01341813919
52	0.4651862072	116	0.0531798177	180	0.01341017657
54	0.4423845534	118	0.048741345		
56	0.4201407032	120	0.04463103284		
58	0.3985026152	122	0.04083716682		
60	0.3775098909	124	0.03734836653		
62	0.3571941868	126	0.03415346256		

Figure 6.4: Directive gain simulated in ANSYS HFSS

BIBLIOGRAPHY

[1] L. C. G. Lázaro, "Analysis and design of mhz-range wireless power transfer systems for implantable devices," 2013.

[2] X. Wei, Z. Wang, and H. Dai, "A critical review of wireless power transfer via strongly coupled magnetic resonances," *energies*, vol. 7, no. 7, pp. 4316–4341, 2014.

[3] A. Somov and R. Giaffreda, "Powering iot devices: Technologies and opportunities," *IEEE IoT Newsletter*, vol. 367, p. 368, 2015.

[4] "Propagation | RF Design Guide | CIRCUIT DESIGN, INC. — cdt21.com," https://www.cdt21.com/design_guide/propagation/, [Accessed 13-01-2025].

[5] S. Chandrasekhar Nambiar, "Design of a wireless power transfer system using electrically coupled loop antennas," Ph.D. dissertation, Virginia Tech, 2015.

[6] S.-H. Hwang, C. G. Kang, Y.-H. Son, and B.-J. Jang, "Software-based wireless power transfer platform for various power control experiments," *Energies*, vol. 8, no. 8, pp. 7677–7689, 2015.

[7] Y. D. Chong, "Complex methods for the sciences," LibreTexts Physics, 2025. [Online]. Available: https://phys.libretexts.org/Bookshelves/Mathematical_Physics_and_Pedagogy/Complex_Methods_for_the_Sciences_(Chong)

[8] R. Paschotta, "Optical intensity," RP Photonics Encyclopedia, 2008. [Online]. Available: https://www.rp-photonics.com/optical_intensity.html

[9] R. C. Johnson and H. Jasik, "Antenna engineering handbook," *New York*, 1984.